Effective e-gasoline production via CO_2-modified Fischer-Tropsch Synthesis

Alessio Tauro [a], Fabrizio Celoria [a], Marco Pietro Mezzapesa [a], Fabio Salomone *[a], Luca Nodari [b], Luca Romagnoletti [c], Emanuele Felli [d], Raffaele Pirone [a], Samir Bensaid *[a]

[a] *Department of Applied Science and Technology (DISAT), Politecnico di Torino, Corso Duca degli Abruzzi 24, 10129 Torino, Italy.*

[b] *Institute of Condensed Matter Chemistry and Technologies for Energy (ICMATE), National Research Council, Corso Stati Uniti 4, 35127 Padua, Italy.*

[c] *API Raffineria di Ancona S.p.A., Via Flaminia 685, 60015 Falconara Marittima, Italy.*

[d] *Italiana Petroli S.p.A., Via Salaria 1322, 00138 Rome, Italy.*

* *Corresponding authors.*

E-mail addresses: fabio.salomone@polito.it, samir.bensaid@polito.it

Supplementary Materials

1. Methodology

1.1 Test Bench Scheme

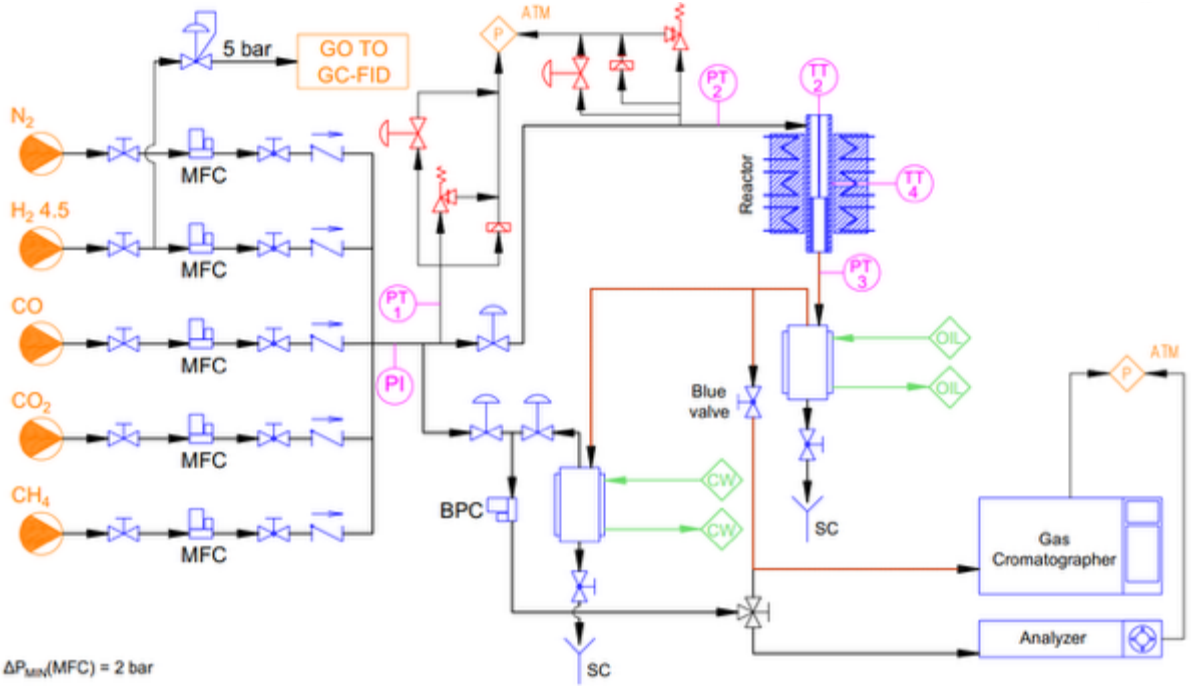

Figure S1. Scheme of the experimental test bench used for pretreatments and catalytic tests.

2. Characterization of the Fresh and Pretreated Samples

2.1 CD_3CN FT-IR and NH_3-TPD Measurements

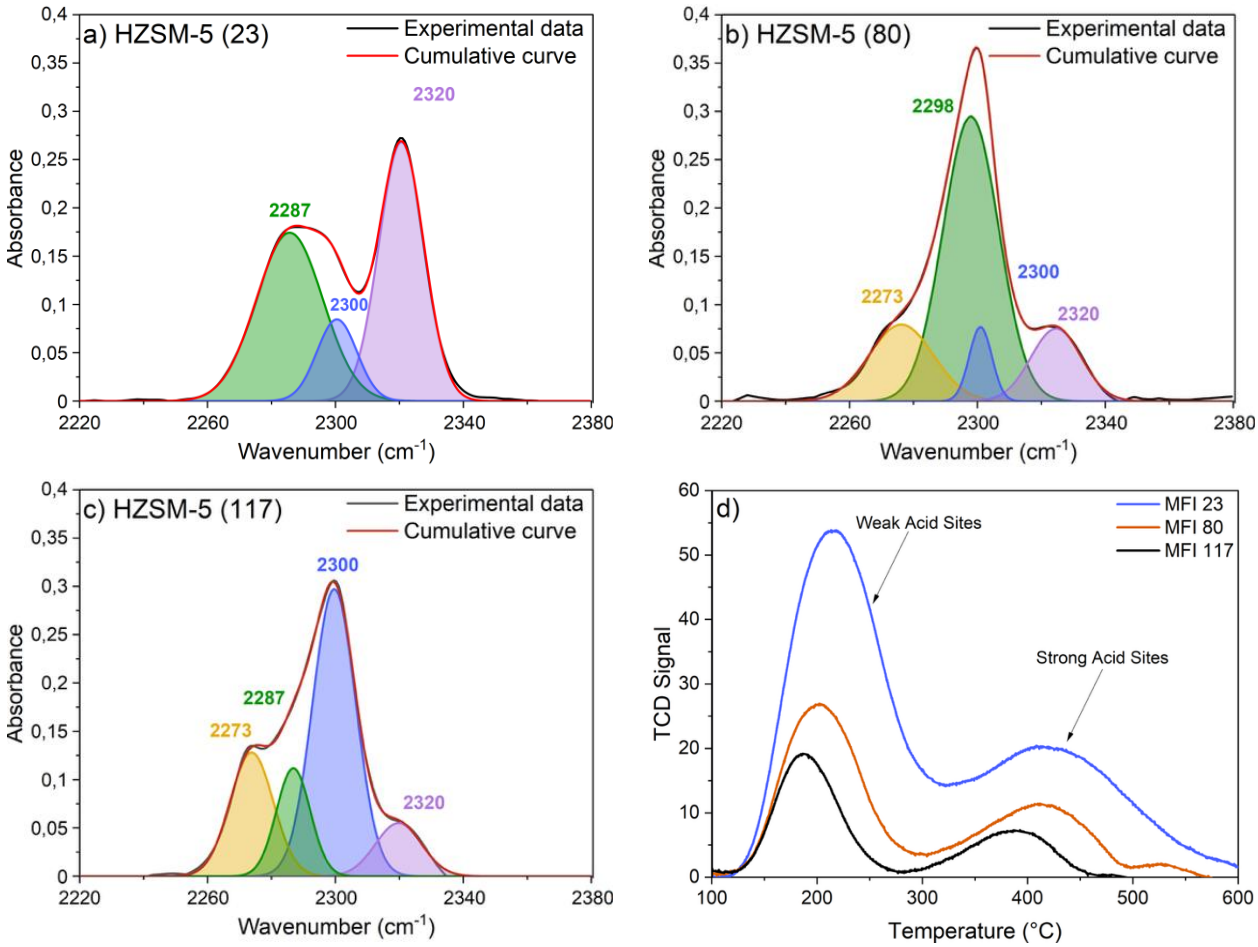

Figure S2. Absorbance profiles of MFI-type zeolites with different SiO_2/Al_2O_3 ratios: (a) 23, (b) 80 and (c) 117. (d) NH_3-TPD profiles.

2.2 N_2-Physisorption Measurements

The results of the N_2-physisrption measurements are reported in TableS1, where SSA_{BET} is the specific surface area evaluated according to the Brunauer-Emmett-Teller (BET) method, SSA_{micro} is the specific surface area of micropores evaluated according to the t-plot method, V_{BJH} is the volume of pores from 1.7 to 300 nm evaluated using the Barrett-Joyner-Halenda (BJH) algorithm, V_{micro} is the volume of micropores and D_{pore} is the average pore diameter.

Table S1. Results of the N_2-physisorption measurements on fresh samples.

Catalyst	SSA_{BET} (m^2/g)	SSA_{micro} (m^2/g)	V_{BJH} (cm^3/g)	V_{micro} (cm^3/g)	D_{pore} (nm)
5%wt. Na-Fe_3O_4	62	1.8	0.150	0.0003	7.2
MFI-23	288	238	0.054	0.125	5.4
MFI-80	394	220	0.118	0.117	3.8
MFI-117	280	203	0.065	0.107	4.4

2.3 X-Ray Diffraction (XRD) Measurements

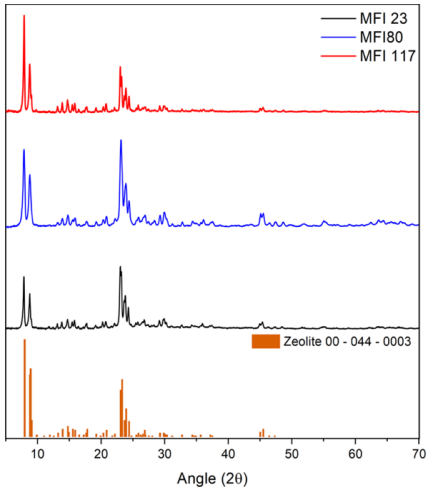

Figure S3. X-ray diffractograms of fresh MFI-type zeolites with different SiO_2/Al_2O_3 molar ratios.

2.4 Scanning Electron Microscopy (SEM) Measurements

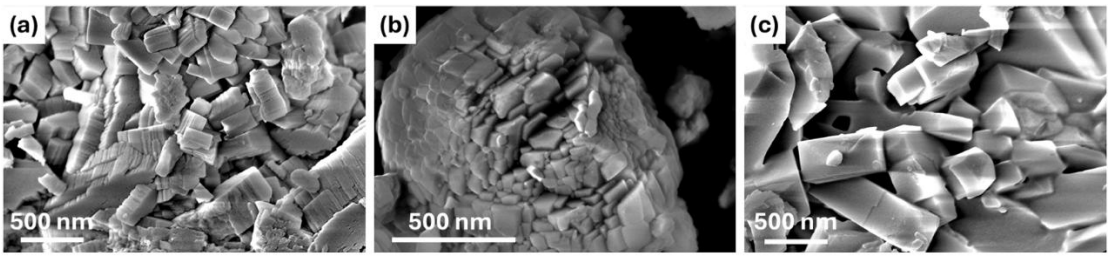

Figure S4. HR SEM images of the fresh MFI-type zeolites: (a) MFI-23, (b) MFI-80 and (c) MFI-117.

2.5 Mössbauer Spectroscopy

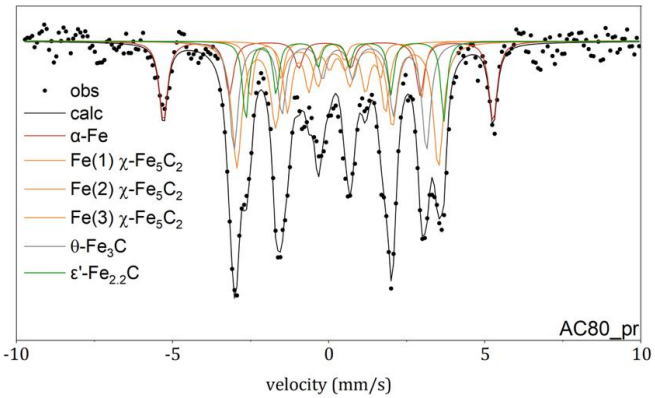

Figure S5. Mössbauer spectrum of the pretreated AC80 sample (AC80_pr).

Table S2. Room temperature hyperfine parameters. δ is quoted relative to α-Fe foil. The errors are estimated as 0.01 mm/s for δ, Δ/ε and Γ_+ , 0.1 T for B and 4% for the relative area.

Sample	δ (mm/s)	Δ/ε (mm/s)	Γ_+ (mm/s)	B (T)	A (%)	Attributions
AC80_pr	-0.066(33)	0.055(33)	0.158(40)	32.74(18)	16	$\alpha - \mathrm{Fe}$
	0.231(42)	0.058(49)	0.192(60)	20.02(23)	29	χ-Fe_5C_2, (Fe1)
	0.154(36)	0.083(37)	0.12*	17.03(31)	9	χ-Fe_5C_2, (Fe2)
	0.263612*	-0.011(36)	0.157(41)	9.71(28)	13	χ-Fe_5C_2, (Fe3)
	0.171(29)	-0.118(36)	0.165(64)	19.11(24)	22	θ-Fe_3C
	0.339(41)	0.180(42)	0.114(73)	19.69(21)	11	ε'-$Fe_{2.2}C$

2.6 SEM-EDS Measurements

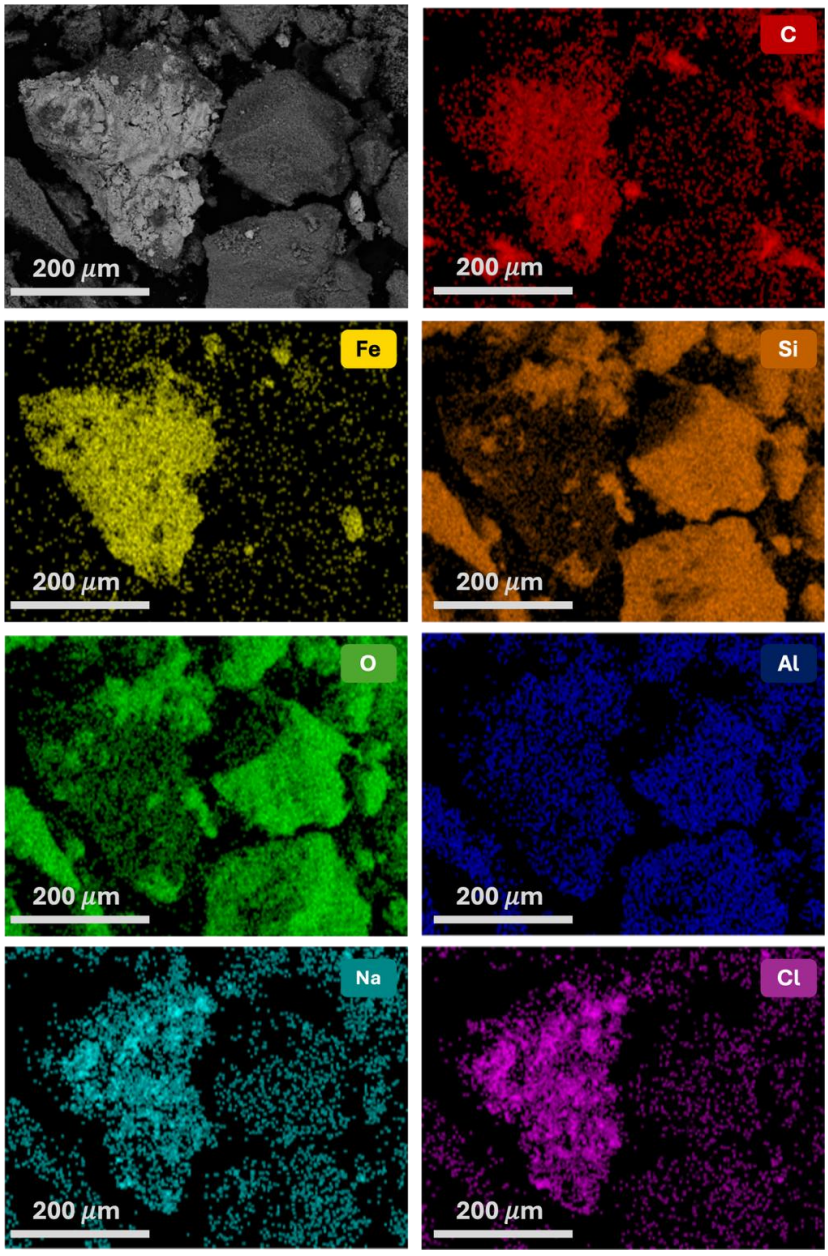

Figure S6. SEM-EDS images of the pretreated AC80 sample (AC80_pr).

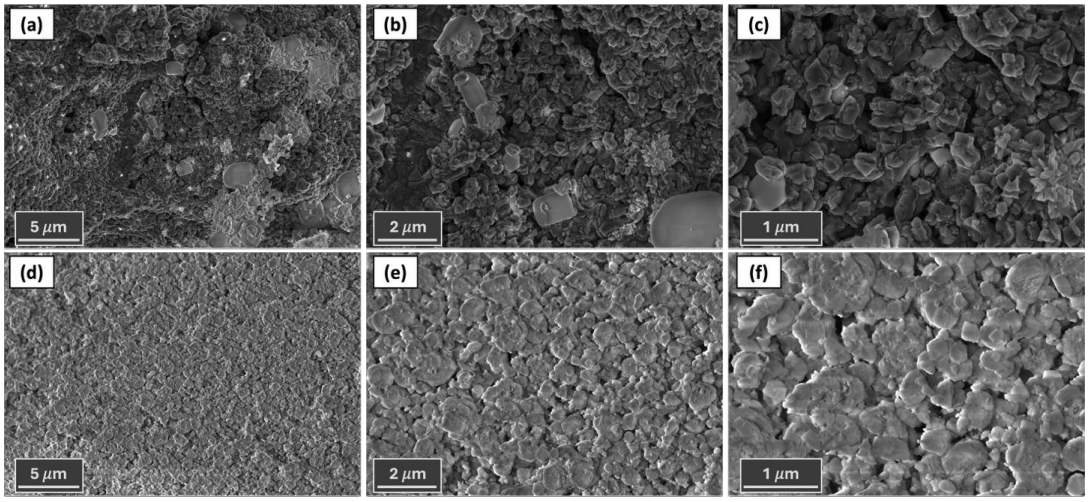

Figure S7. High resolution SEM images of the pretreated AC80 sample (AC80_pr): Fe region with a magnification of (a) 10 kX, (b) 25 kX and (c) 50 kX; zeolite region with a magnification of (d) 10 kX, (e) 25 kX and (f) 50 kX.

2.7 Transmission Electron Microscopy (TEM) Measurements

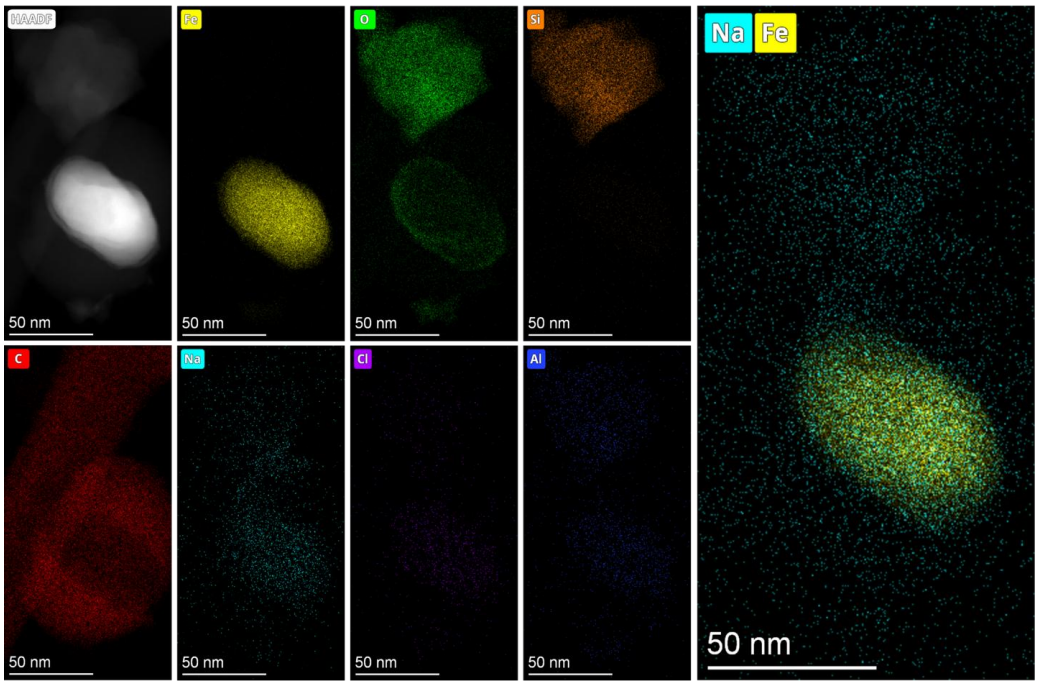

Figure S8. STEM-EDS images of the pretreated AC80 sample (AC80_pr).

3. Catalytic results

Table S3. Catalytic performance of all samples ($H_2/CO_2/N_2$ = 15/5/3, 7 NL·g$Fe_3O_4^{-1}$·h^{-1}, 23 bar, 2 g Na/Fe_3O_4, 2 g zeolite).

Sample	T (°C)	TOS (h)	ζ_{CO_2} (%)	σ_{CO} (%)	CO-free product selectivity (%)														$\eta_{C_{6+}}$ (%)	η_{HC} (%)
					σ_{CH_4}	σ_{DME}	σ_{CH_3OH}	$\sigma_{C_{2=}}$	$\sigma_{C_{2-}}$	$\sigma_{C_{3=}}$	$\sigma_{C_{3-}}$	$\sigma_{C_{4=}}$	$\sigma_{C_{4-}}$	$\sigma_{C_{5=}}$	$\sigma_{C_{5-}}$	$\sigma_{C_{6+}}$	$\sigma_{C_{2=/5=}}$	$\sigma_{C_{2-/5-}}$		
A23	360	24	34.6	18.6	18.8	0.0	0.1	1.7	2.7	3.1	15.5	17.6	7.8	8.6	2.7	21.4	25.2	23.3	6.0	28.1
	380	12	43.6	18.9	28.1	0.0	0.1	2.0	3.1	3.1	12.7	14.6	6.4	6.9	2.2	20.9	21.5	19.8	7.4	35.3
	360	54	41.2	18.0	24.7	0.0	0.2	2.3	2.9	4.0	9.0	15.9	6.5	7.9	3.4	23.2	24.7	17.9	7.8	33.8
A80	360	24	43.5	13.8	17.4	0.0	0.2	0.9	2.6	1.6	10.9	17.3	7.0	10.4	2.5	29.1	26.1	19.8	10.9	37.5
	380	12	47.5	16.5	27.6	0.0	0.6	1.2	3.0	1.9	9.4	14.7	6.0	8.1	2.1	25.5	21.6	17.1	10.1	39.7
	360	72	42.6	17.9	23.9	0.0	0.2	1.7	2.7	2.9	7.5	15.6	6.2	9.0	3.2	27.0	24.1	16.1	9.4	34.9
A117	360	24	31.3	17.1	17.7	0.0	0.5	2.0	3.0	3.9	11.7	18.5	8.1	10.9	3.7	20.0	29.3	22.0	5.2	26.0
	380	12	39.0	18.4	26.0	0.0	0.2	2.7	3.2	4.1	10.0	15.5	6.7	9.0	3.0	19.6	25.5	18.6	6.3	31.8
	360	60	29.5	23.2	27.6	0.0	0.3	3.2	3.5	4.5	8.4	15.6	6.6	9.8	3.7	16.9	25.3	17.1	3.8	22.6
AC23	360	30.5	40.5	12.9	24.8	0.0	0.0	0.7	3.0	1.0	13.6	17.4	7.3	9.2	2.0	21.0	24.6	22.6	7.4	35.3
	380	13.5	39.4	19.9	40.5	0.0	0.0	1.1	4.1	1.5	10.3	13.9	5.9	7.6	1.8	13.3	19.3	17.8	4.2	31.5
	340	10.5	29.2	24.1	32.0	0.0	0.0	1.4	3.9	1.9	8.0	15.4	6.1	9.4	2.9	19.0	21.3	15.9	4.2	22.1
	360	48	34.1	23.5	41.7	0.0	0.0	1.5	4.4	1.9	7.5	13.3	5.2	7.8	2.2	14.4	18.8	14.8	18.8	26.1
AC80	360	21	43.9	11.1	22.7	0.0	0.7	0.8	2.9	1.5	11.2	16.4	7.0	10.1	2.3	24.3	25.6	20.8	9.5	39.0
	380	11	44.3	13.2	32.5	0.0	0.0	1.4	3.5	2.2	8.7	14.6	5.8	8.4	2.2	20.5	23.2	17.6	7.9	38.5
	340	16.5	36.8	14.8	21.7	0.0	0.0	1.8	2.7	3.0	7.1	15.9	6.5	10.0	3.6	27.7	26.2	16.9	8.7	31.3
	360	30.5	37.8	28.1	19.0	0.0	0.0	2.1	3.2	3.6	7.5	16.2	6.4	9.8	3.3	19.8	25.6	16.6	6.1	28.7
AC117	360	17	32.0	16.7	25.0	0.0	0.0	1.3	3.1	2.6	10.3	18.1	7.4	11.1	3.1	18.1	27.6	19.9	4.8	26.7
	380	9.5	42.4	30.3	20.0	0.0	0.4	1.3	3.4	2.5	8.3	14.1	5.7	8.4	2.3	23.2	21.1	15.7	7.9	34.0
	340	14	31.6	24.2	23.3	0.0	0.6	1.7	3.4	3.1	7.6	15.2	6.7	10.6	3.9	24.1	23.1	16.3	5.8	24.0
	360	20	34.5	19.7	29.9	0.0	0.5	1.9	3.6	3.2	7.2	13.9	5.9	9.5	3.1	21.4	22.8	15.9	5.9	27.7
AC80_DB	360	42	35.0	15.5	24.5	0.0	0.1	1.6	3.3	2.5	10.6	18.8	8.5	15.4	0.3	14.3	32.4	19.1	4.2	29.5

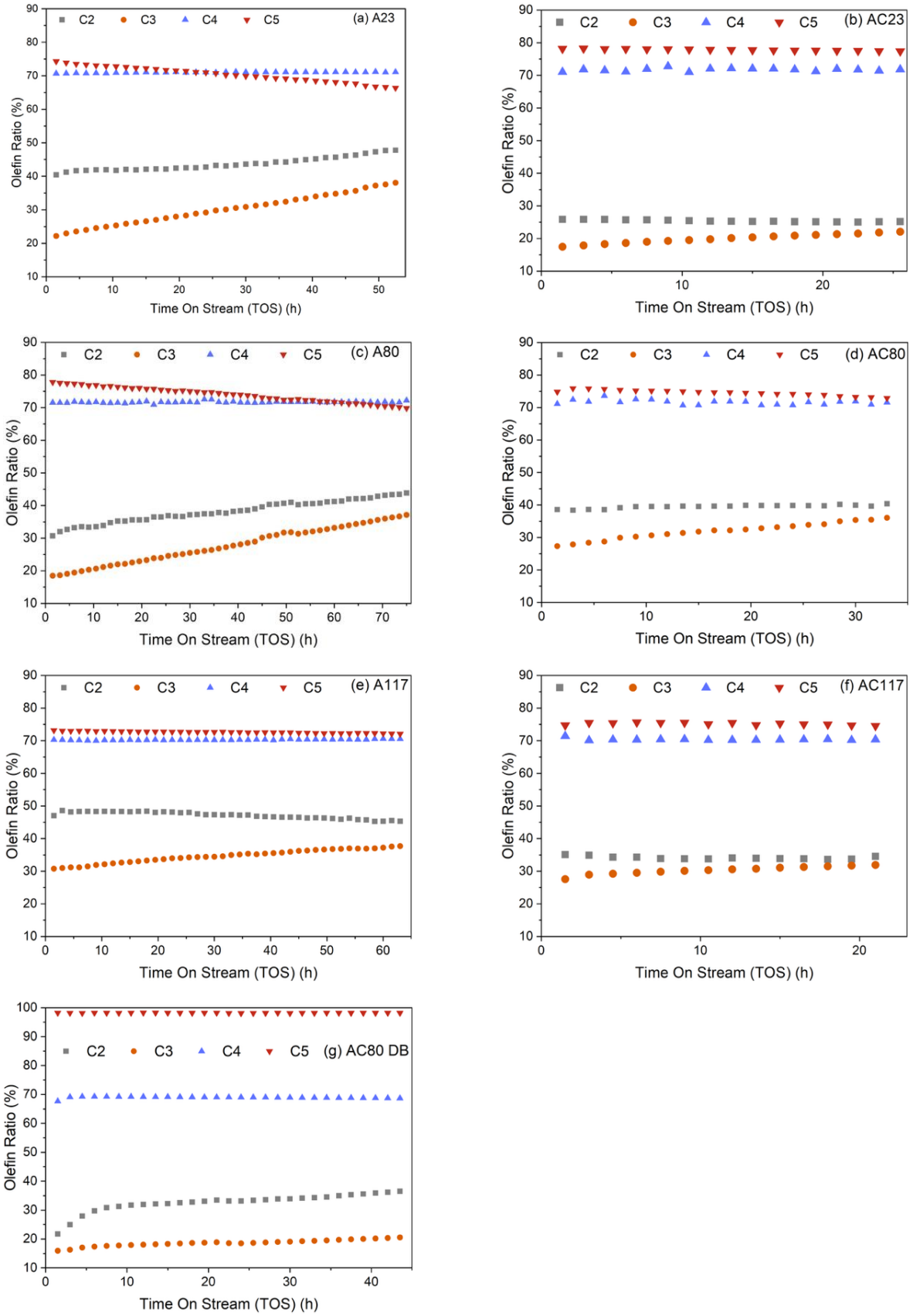

Figure S9. Olefin content for each carbon atom components in the gas phase during time on stream. Reaction conditions: 7 $NL \cdot gFe_3O_4^{-1} \cdot h^{-1}$ ($H_2/CO_2/N_2$ = 15/5/3), 360°C, 23 bar, 2 g Na/Fe_3O_4, 2 g zeolite. Samples: (a) A23, (b) AC23, (c) A80, (d) AC80, (e) A117, (f) AC117 and (g) AC80_DB.

4. Characterization of spent samples

4.1 X-Ray Diffraction Measurements

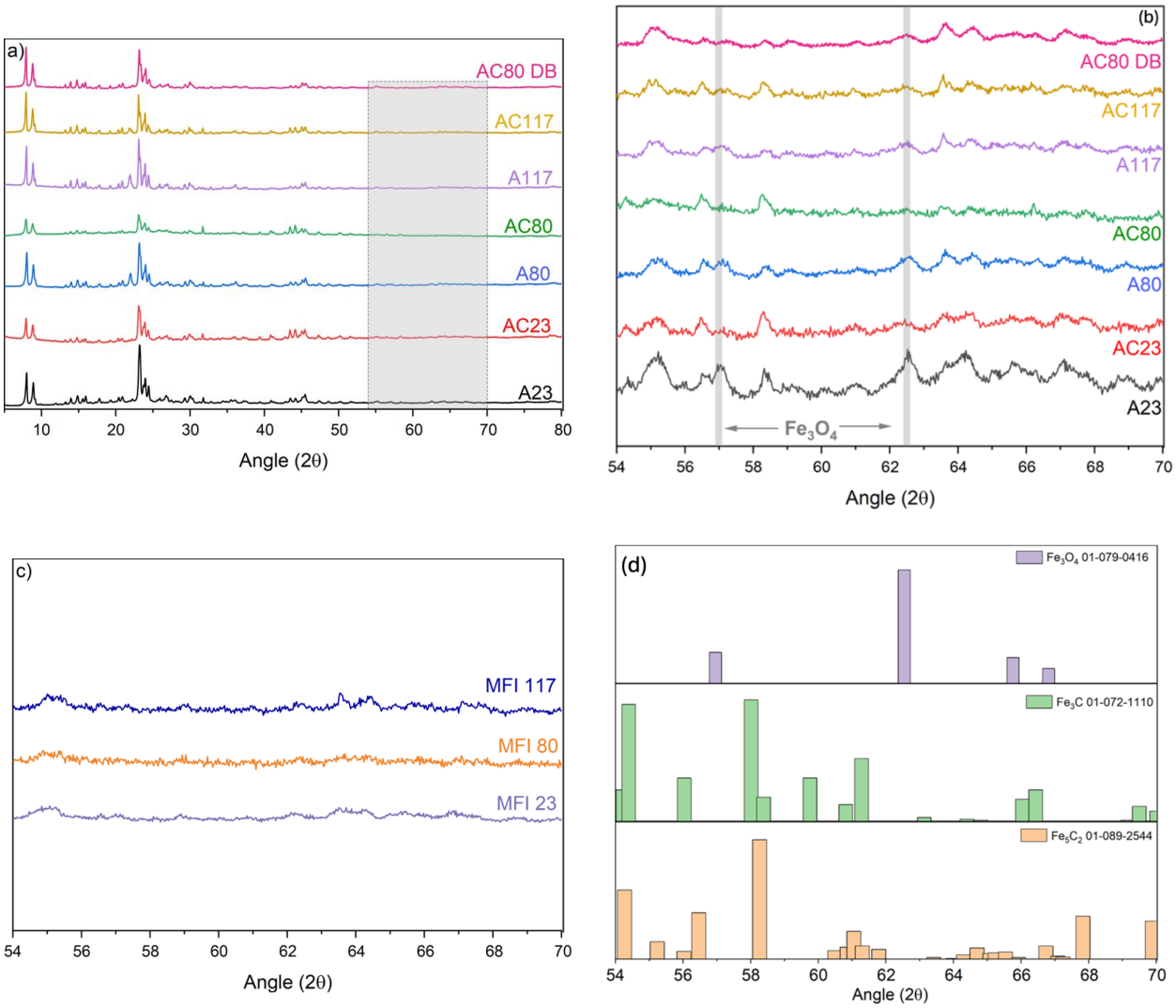

Figure S10. (a) X-ray diffractograms of all spent samples collected over the 5°-80° 2θ range. Magnified view of the 54°-70° 2θ range for (b) spent samples and (c) parent zeolites. (d) Reference diffraction patterns of magnetite and iron carbides in 54°-70° 2θ range.

4.2 Mössbauer Spectroscopy

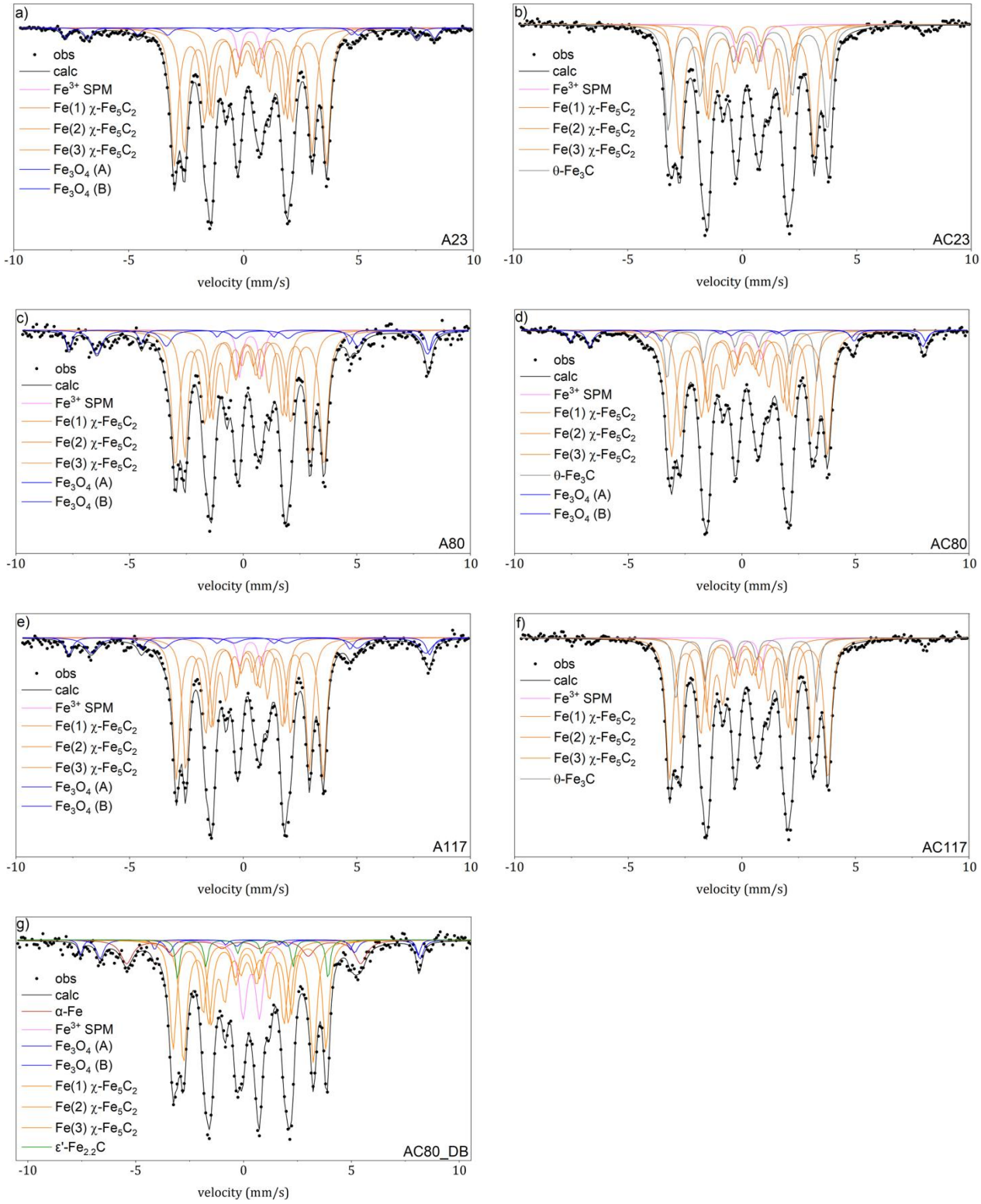

Figure S11. Mössbauer spectra of the spent samples: (a) A23, (b) AC23, (c) A80, (d) AC80, (e) A117, (f) AC117, and (g) AC80_DB.

Table S4. Room temperature hyperfine parameters. δ is quoted relative to α-Fe foil. The errors are estimated as 0.01 mm/s for δ, Δ/ε and Γ_+ , 0.1 T for B and 4% for the relative area.

Sample	δ (mm/s)	Δ/ε (mm/s)	Γ_+ (mm/s)	B (T)	A (%)	Attributions
A23	0.303(16)	1.004(30)	0.133(23)	-	3	SPM Fe^{3+} NPs
	0.2594(37)	0.0429(36)	0.1936(65)	20.528(27)	37	χ-Fe_5C_2, (Fe1)
	0.1730(49)	0.0317(49)	0.1867(72)	17.253(28)	33	χ-Fe_5C_2, (Fe2)
	0.2233(58)	0.0519(55)	0.1670(83)	10.123(37)	21	χ-Fe_5C_2, (Fe3)
	0.165(40)	0.113(40)	0.169(38)	49.84(27)	3	Fe_3O_4 (A)
	0.620(44)	-0.227(44)	0.199(41)	44.40(28)	3	Fe_3O_4 (B)
A80	0.326(30)	0.974(57)	0.134(44)	-	4	SPM Fe^{3+} NPs
	0.247(11)	0.044(11)	0.205(19)	20.284(82)	37	χ-Fe_5C_2, (Fe1)
	0.160(12)	0.028(12)	0.173(19)	17.090(75)	29	χ-Fe_5C_2, (Fe2)
	0.238(16)	0.037(15)	0.161(23)	9.99(11)	18	χ-Fe_5C_2, (Fe3)
	0.180(56)	0.075(57)	0.135(82)	49.14(42)	4	Fe_3O_4 (A)
	0.834(73)	0.003(75)	0.26(12)	45.15(53)	8	Fe_3O_4 (B)
A117	0.323561*	0.939(51)	0.144(40)	-	3	SPM Fe^{3+} NPs
	0.2546(51)	0.0375(51)	0.1866(88)	20.038(38)	36	χ-Fe_5C_2, (Fe1)
	0.1720(66)	0.0253(65)	0.1721(95)	16.879(37)	31	χ-Fe_5C_2, (Fe2)
	0.2134(88)	0.0547(85)	0.156(12)	9.822(54)	19	χ-Fe_5C_2, (Fe3)
	0.190(40)	0.079(41)	0.180(64)	49.24(28)	4	Fe_3O_4 (A)
	0.722(63)	-0.044(65)	0.33(12)	45.67(43)	7	Fe_3O_4 (B)
AC23	0.307(20)	0.998(36)	0.173(30)	-	4	SPM Fe^{3+} NPs
	0.344(16)	0.0675(94)	0.128(22)	21.351(62)	10	χ-Fe_5C_2, (Fe1)
	0.1766(65)	0.0304(64)	0.1979(95)	18.215(38)	35	χ-Fe_5C_2, (Fe2)
	0.2220(73)	0.0532(71)	0.177(10)	10.758(49)	22	χ-Fe_5C_2, (Fe3)
	0.21	0.00358(71)	0.194(13)	21.545(46)	28	θ-Fe_3C
AC80_pr	-0.066(33)	0.055(33)	0.158(40)	32.74(18)	16	$\alpha - \mathrm{Fe}$
	0.231(42)	0.058(49)	0.192(60)	20.02(23)	29	χ-Fe_5C_2, (Fe1)
	0.154(36)	0.083(37)	0.12*	17.03(31)	9	χ-Fe_5C_2, (Fe2)
	0.263612*	-0.011(36)	0.157(41)	9.71(28)	13	χ-Fe_5C_2, (Fe3)
	0.171(29)	-0.118(36)	0.165(64)	19.11(24)	22	θ-Fe_3C
	0.339(41)	0.180(42)	0.114(73)	19.69(21)	11	ε'-$Fe_{2.2}C$
AC80	0.340(20)	1.048(38)	0.161(31)	-	3	SPM Fe^{3+} NPs
	0.2795(57)	0.0658(57)	0.2150(84)	21.277(41)	36	χ-Fe_5C_2, (Fe1)
	0.1692(68)	0.0249(68)	0.1844(100)	17.892(47)	26	χ-Fe_5C_2, (Fe2)
	0.2249(77)	0.0415(75)	0.188(11)	10.718(58)	20	χ-Fe_5C_2, (Fe3)
	0.1128(96)	-0.1061(98)	0.12*	20.423(62)	8	θ-Fe_3C
	0.290(39)	-0.013(40)	0.150(63)	48.53(27)	2	Fe_3O_4 (A)
	0.670(31)	-0.028(32)	0.180(50)	45.47(21)	4	Fe_3O_4 (B)
AC80_DB	0.359(23)	0.763(47)	0.208(33)	-	9	SPM Fe^{3+} NPs
	-0.066(96)	0.073(93)	0.33(12)	33.64(47)	9	$\alpha - \mathrm{Fe}$
	0.230(26)	0.049(14)	0.179(31)	21.98(11)	23	χ-Fe_5C_2, (Fe1)
	0.181(13)	0.048(13)	0.192(20)	18.672(81)	28	χ-Fe_5C_2, (Fe2)
	0.233(18)	0.067(17)	0.192(25)	11.07(12)	18	χ-Fe_5C_2, (Fe3)
	0.349523*	-0.065(65)	0.114(92)	48.58(50)	2	Fe_3O_4 (A)
	0.814(77)	-0.044(75)	0.19(11)	46.00(50)	4	Fe_3O_4 (B)
	0.357(38)	0.077(27)	0.107(70)	21.65(21)	5	$\varepsilon' - \mathrm{Fe}_{2.2}\mathrm{C}$
AC117	0.327(15)	1.052(29)	0.132(23)	-	3	SPM Fe^{3+} NPs
	0.2557(35)	0.0468(34)	0.1806(60)	21.642(28)	38	χ-Fe_5C_2, (Fe1)
	0.1652(47)	0.0435(47)	0.1479(96)	17.913(57)	24	χ-Fe_5C_2, (Fe2)
	0.2389(58)	0.0687(54)	0.1665(79)	10.738(43)	22	χ-Fe_5C_2, (Fe3)
	0.1857(77)	0.0165(76)	0.125(19)	19.236(77)	13	θ-Fe_3C

*Fixed Parameters

4.3 Transmission Electron Microscopy (TEM) Measurements

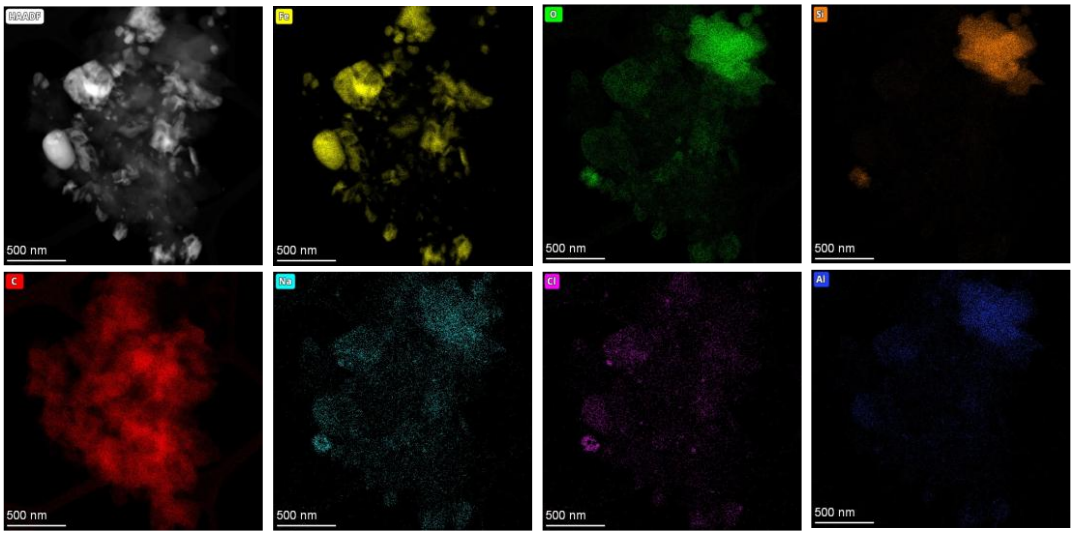

Figure S12. STEM-EDS images of the spent AC23 sample.

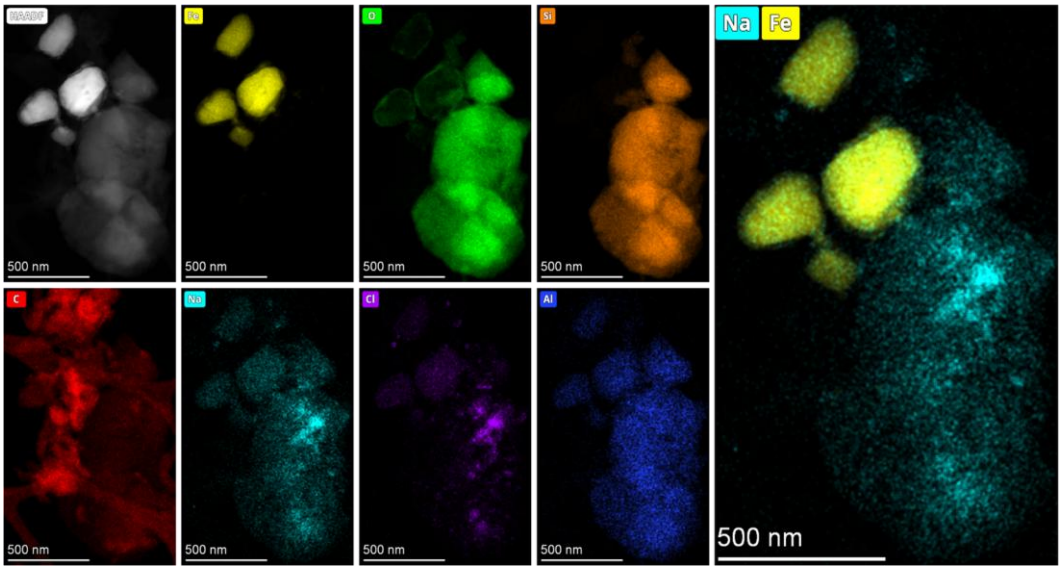

Figure S13. STEM-EDS images of the spent AC80 sample.

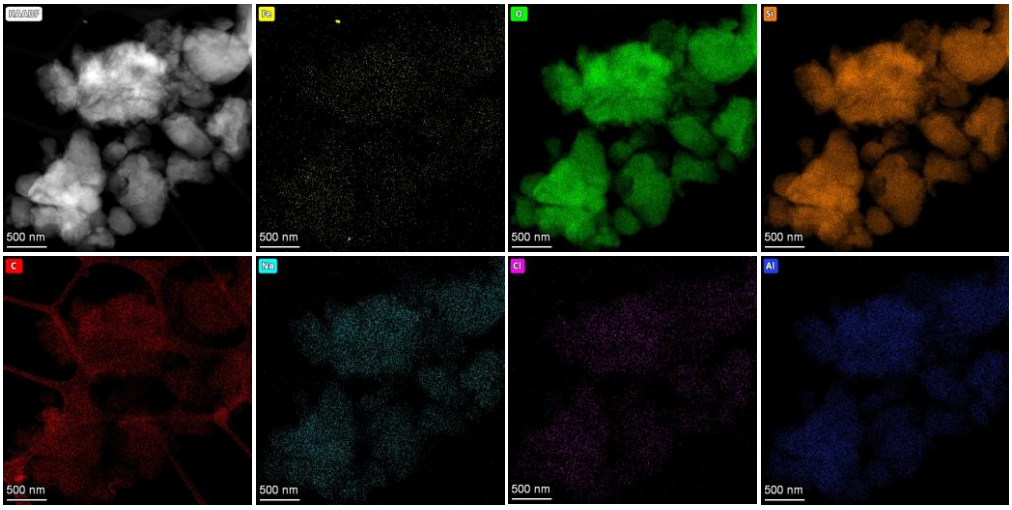

Figure S14. STEM-EDS images of the spent AC80_DB sample.

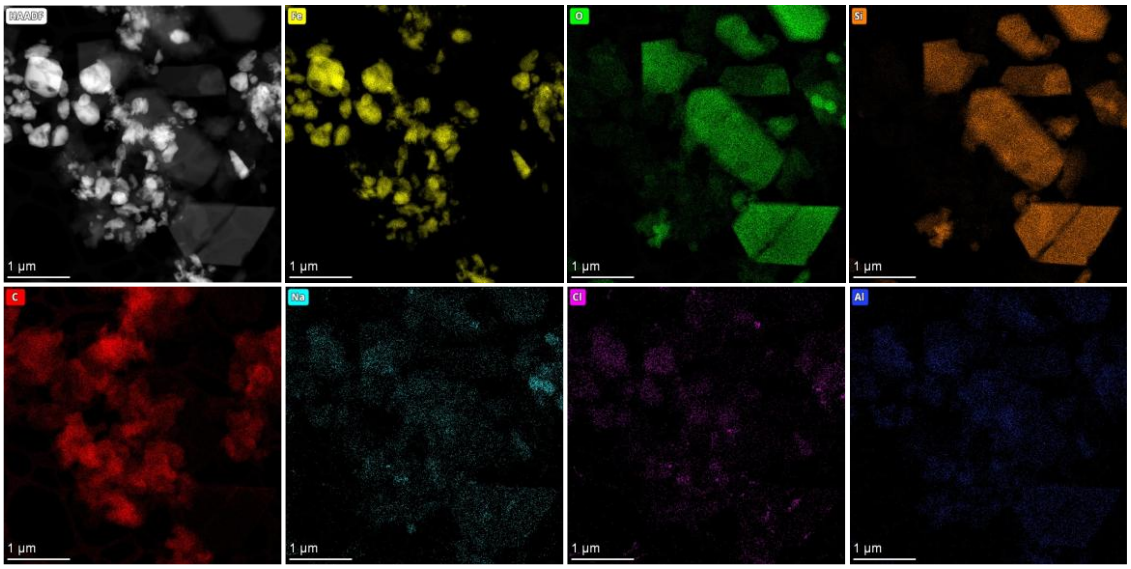

Figure S15. STEM-EDS images of the spent AC117 sample.

Table S5. STEM-EDS elemental quantification on pretreated and spent AC-treated samples.

Sample	Nominal Si/Al	Si/Al (at. %)	Si/Al/Na (at. %)	Na/Al (at. %)	Migrated Na ($mmol_{Na}/g_{Zeolite}$)
AC23	11.5	11.6	88.3/7.6/4.11	45	0.610
AC80_pr	40	39.7	96.5/2.43/1.05	43	0.176
AC80	40	38.2	95.1/2.49/2.41	97	0.400
AC80_DB	40	33.1	96.3/2.91/0.78	27	0.111
AC117	58.5	57.1	96.4/1.68/1.9	110	0.305

In Table S3, the Si, Al and Na atomic content were determined by means of STEM-EDS on specific zeolite domains selected from those shown in Figures S11-S14.

4.4 NH_3-TPD Measurements

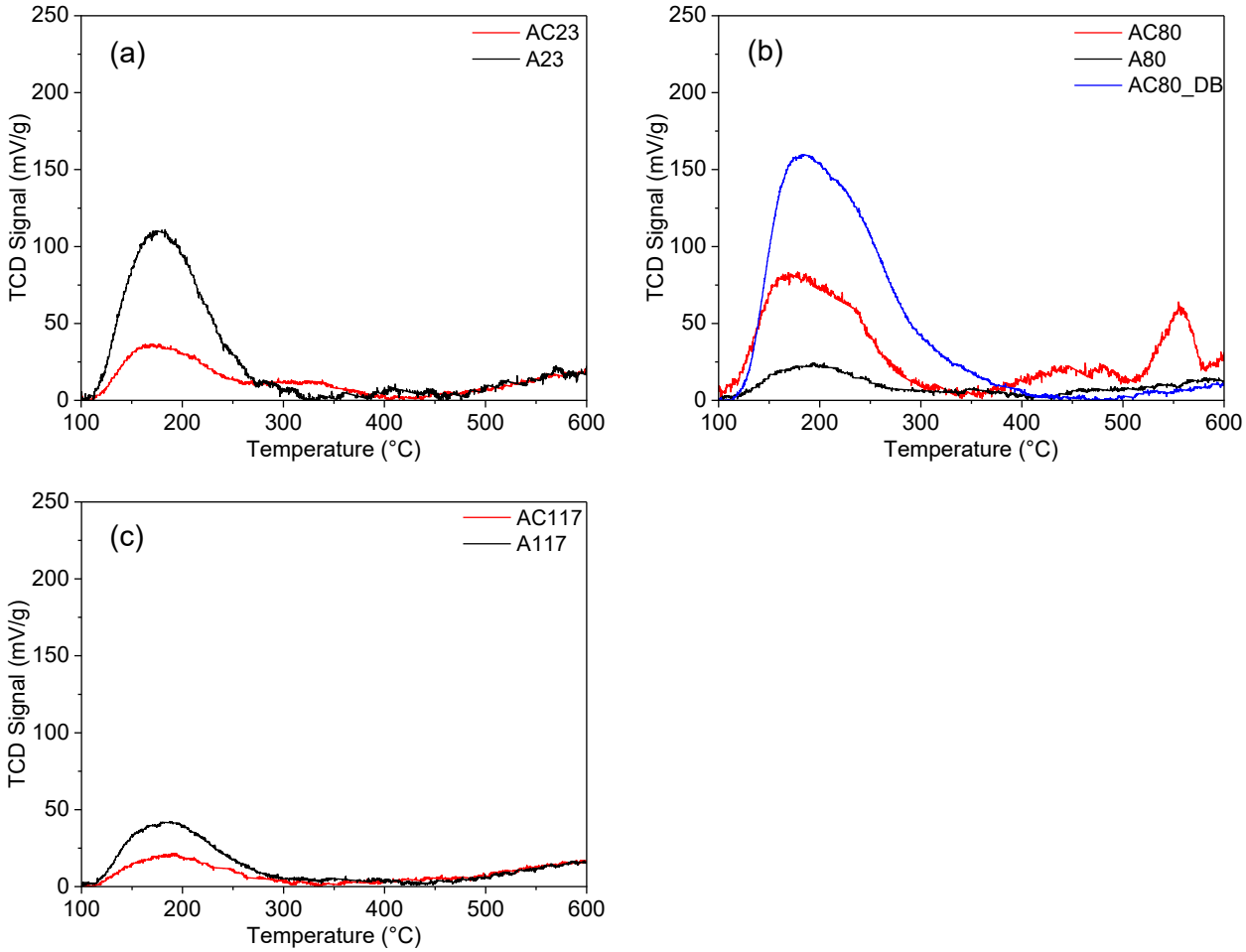

Figure S16. NH3-TPD profiles of the regenerated spent samples: (a) A23 and AC23; (b) A80, AC80 and AC80_DB; (c) A117 and AC117.

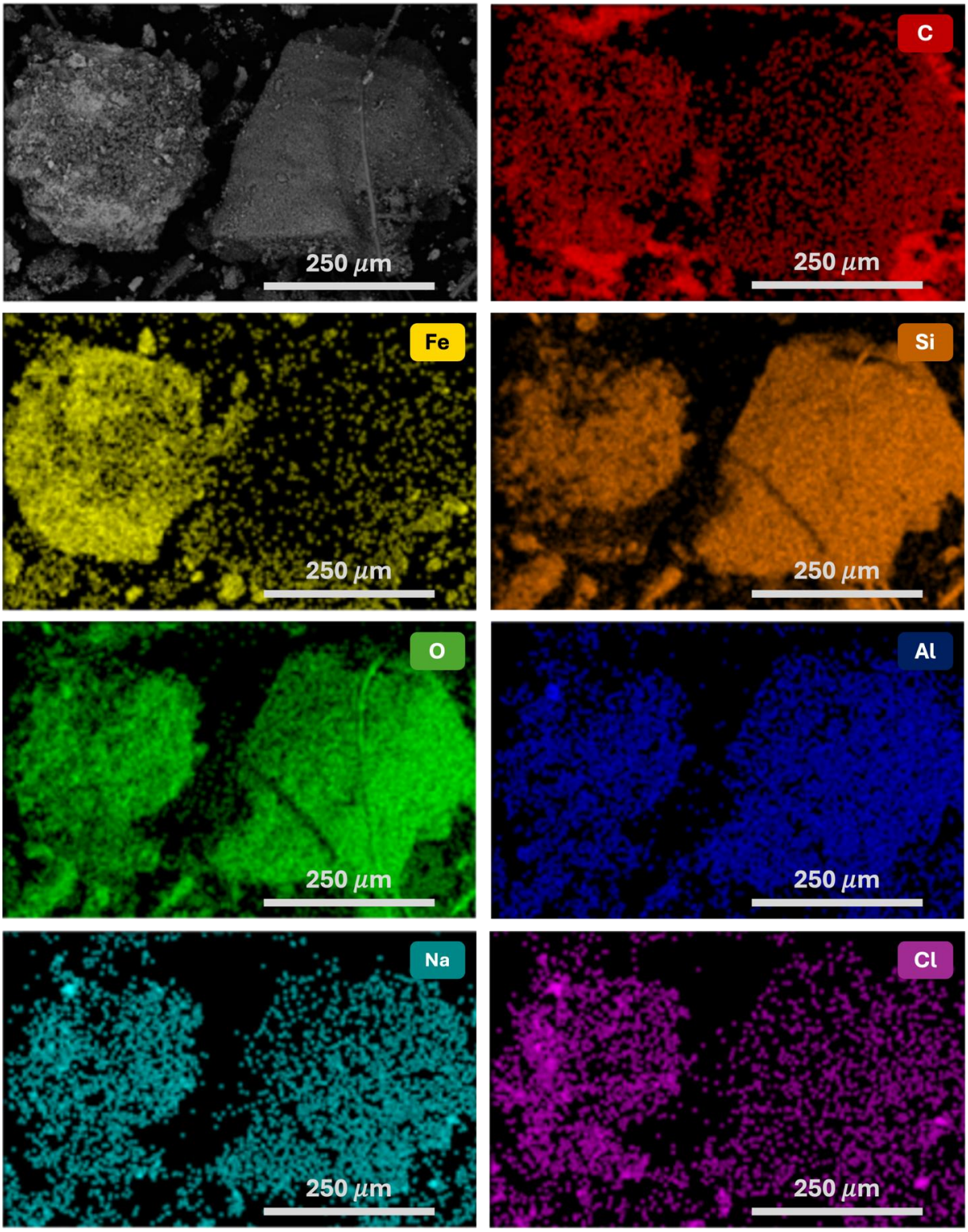

Figure S17. SEM-EDS images of spent sample A80 (area #1).

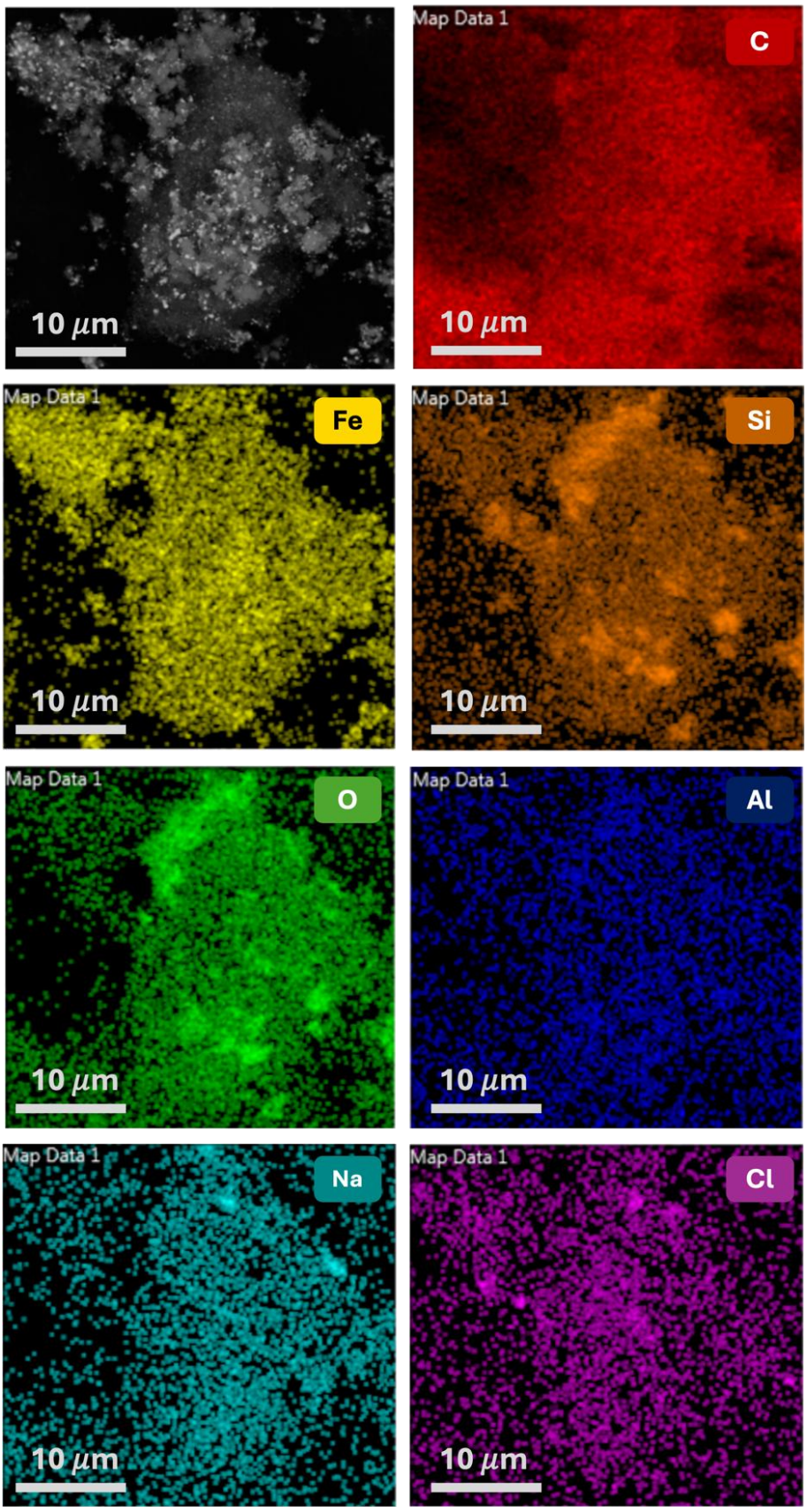

Figure S18. SEM-EDS images of spent sample AC80.

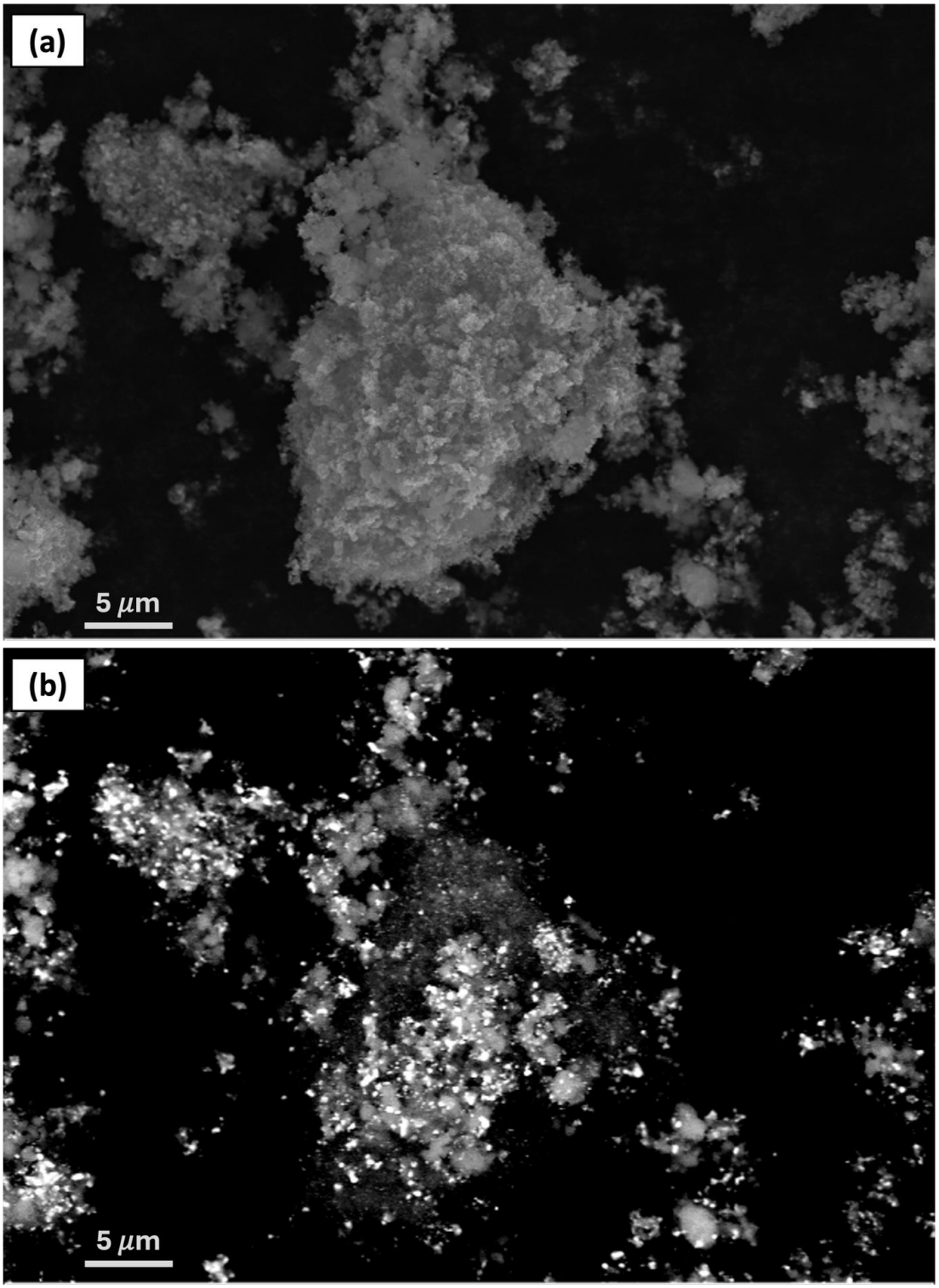

Figure S19. SEM images of spent AC80 sample with a magnification of 5 kX. Images collected with the (a) high resolution detector and the (b) back-scattered electron detector.

4.6 Transmission Electron Microscopy (TEM) Measurements

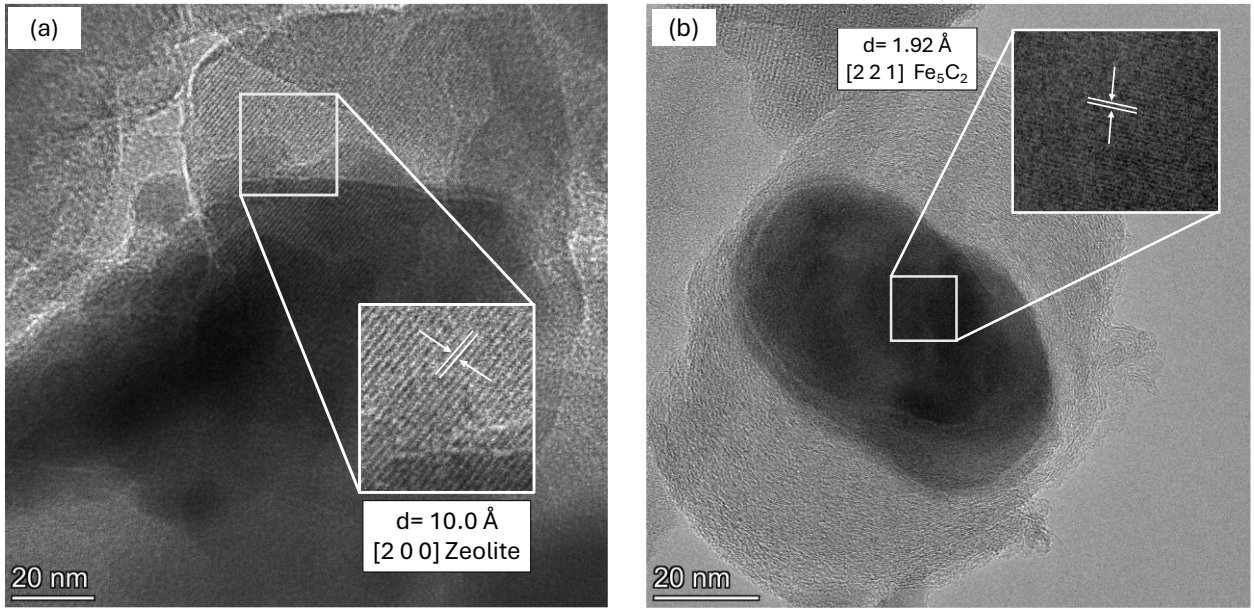

Figure S20. HR-TEM images of the spent AC80 sample and interplanar distances of the (a) MFI-type zeolite and of the (b) Hägg carbide (χ-Fe_5C_2).

5. Liquid Products

5.1 Detailed Hydrocarbon Analysis (DHA)

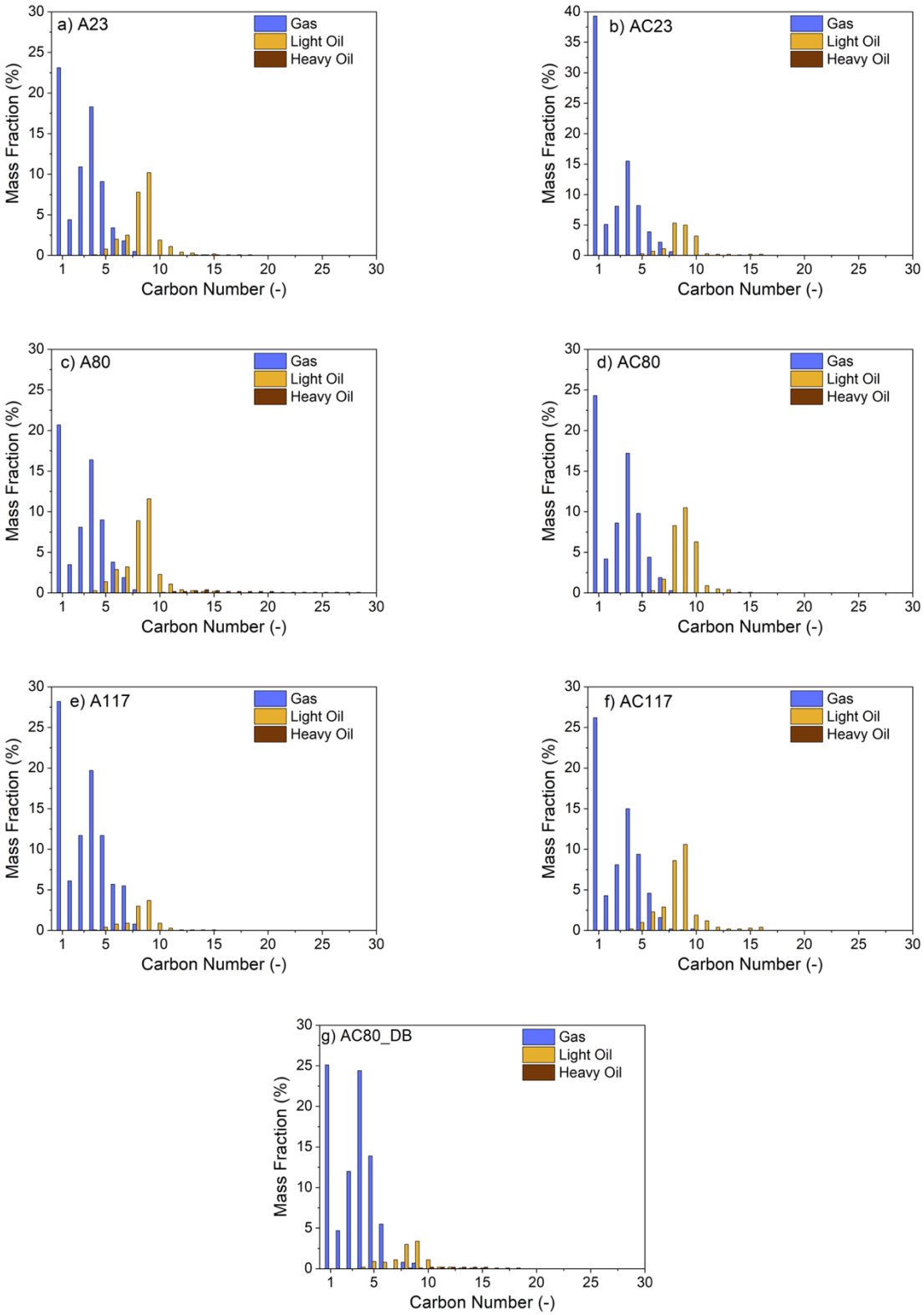

Figure S21. Product distributions grouped by HC class and gas phase, light oil, heavy oil.. Reaction conditions: 7 NL·g$Fe_3O_4^{-1}$·h^{-1} (H_2/CO_2/N_2 = 15/5/3), 360°C, 23 bar, 2 g Na/Fe_3O_4, 2 g zeolite. Samples: (a) A23, (b) AC23, (c) A80, (d) AC80, (e) A117, (f) AC117 and (g) AC80_DB.

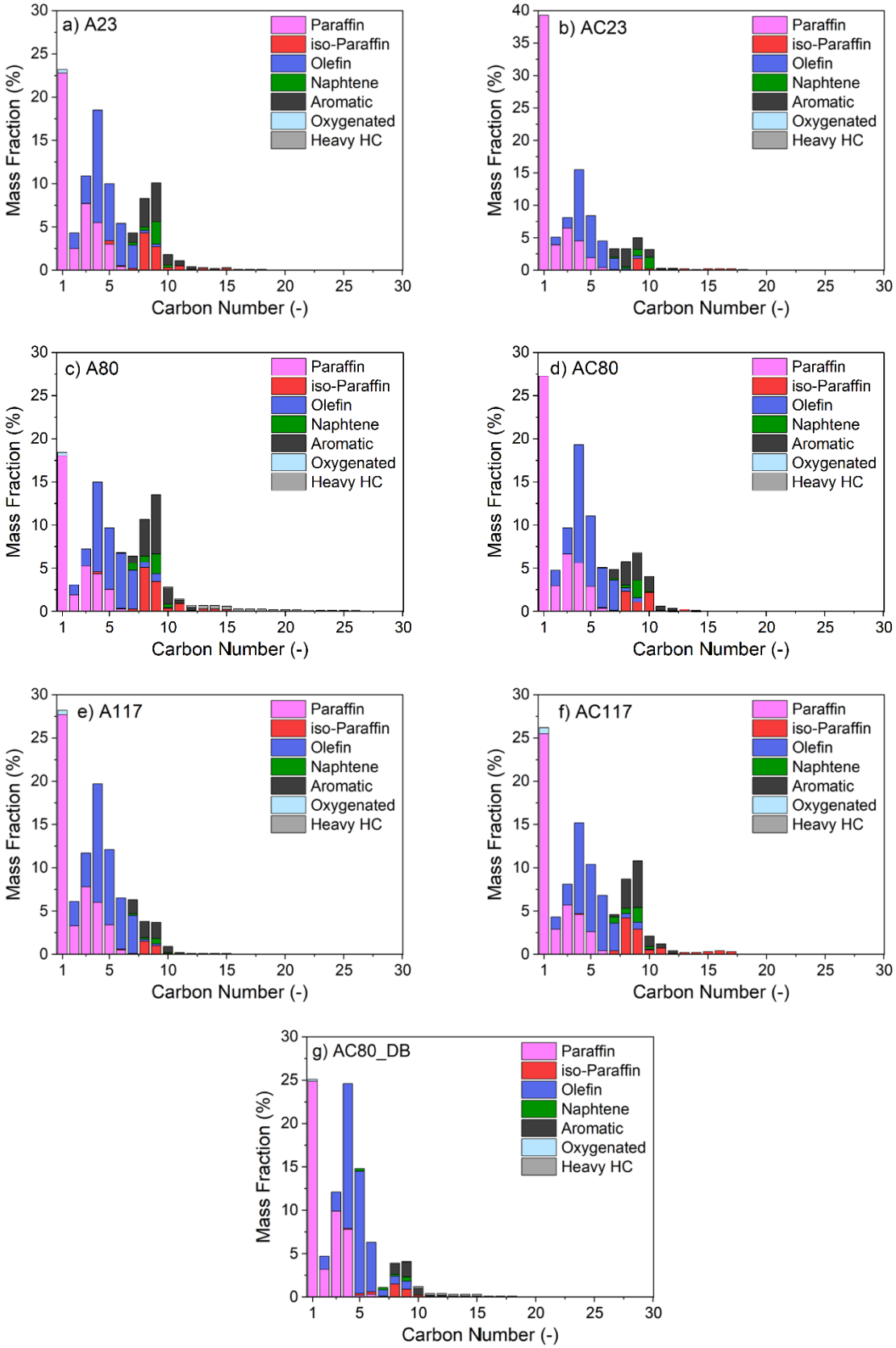

Figure S22. Product distributions grouped by HC classes for the samples: (a) A23, (b) AC23, (c) A80, (d) AC80, (e) A117, (f) AC117 and (g) AC80_DB. Reaction conditions: 7 $NL \cdot gFe_3O_4^{-1} \cdot h^{-1}$ ($H_2/CO_2/N_2$ = 15/5/3), 2.3 MPa, 360 °C, 2 g Na-Fe_3O_4, 2 g zeolite.

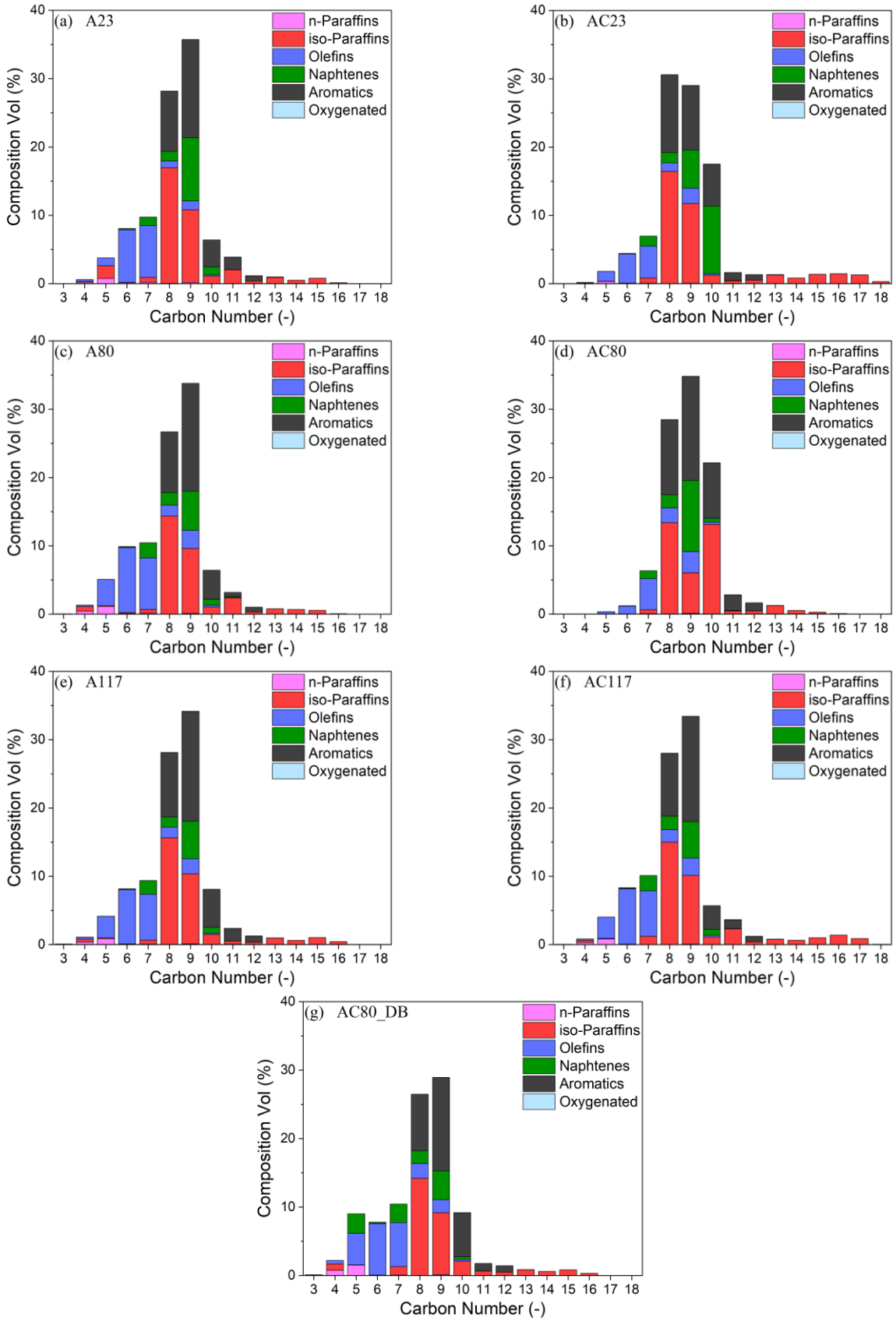

Figure S23. Ligh oil product distributions analyzed by means of DHA for the samples: (a) A23, (b) AC23, (c) A80, (d) AC80, (e) A117, (f) AC117 and (g) AC80_DB. Reaction conditions: 7 NL·g$Fe_3O_4^{-1}$·h^{-1} (H_2/CO_2/N_2 = 15/5/3), 2.3 MPa, 360 °C, 2 g Na-Fe_3O_4, 2 g zeolite.

Table S6. Catalytic performance of all samples ($H_2/CO_2/N_2$ = 15/5/3, 7 NL·g$Fe_3O_4^{-1}$·h^{-1}, 23 bar, 2 g Na/Fe_3O_4, 2 g zeolite).

Sample	T (°C)	Paraffins	iso-Paraffins	Olefins	Naphthenes	Aromatics	Average Cn
A23	360-D	1.36	42.57	15.67	9.41	30.99	8.39
	380	0.48	44.21	11.81	9.75	33.75	8.66
	360	1.99	35.98	21.24	11.55	29.24	8.20
A80	360-D	2.09	31.19	21.11	20.04	25.57	8.27
	380	1.56	38.85	19.48	8.35	31.76	8.29
	360	1.90	31.27	25.56	11.00	30.27	8.22
A117	360-D	1.53	37.80	18.63	9.65	32.39	8.55
	380	1.47	35.68	20.22	9.55	33.08	8.38
	360	1.55	32.34	22.18	10.00	33.93	8.39
AC23	360-D	1.71	41.27	17.34	14.61	25.06	8.45
	380	0.99	43.37	14.78	14.62	26.23	8.67
	340	0.65	36.87	15.81	9.61	37.06	8.88
	360	0.55	37.72	14.18	18.57	28.98	9.00
AC80	360-D	0.09	35.16	10.39	15.15	39.21	8.74
	380	0.76	35.37	15.86	19.54	28.46	8.84
	340	1.72	24.48	25.19	13.99	34.62	8.30
	360	0.20	36.08	11.77	14.07	37.89	8.96
AC117	360-D	1.87	30.17	22.85	14.04	31.08	8.31
	380	1.07	30.10	19.86	14.53	34.44	8.37
	340	0.98	29.76	22.04	11.55	35.67	8.53
	360	1.26	35.20	22.80	10.51	30.23	8.53
AC80_DB	360-D	2.42	31.53	23.37	12.25	30.44	8.12

Table S7. Catalytic performance of all samples ($H_2/CO_2/N_2$ = 15/5/3, 7 NL·g$Fe_3O_4^{-1}$·h^{-1}, 23 bar, 2 g Na/Fe_3O_4, 2 g zeolite).

Sample	T (°C)	Average MW (g/mol)	Specific Gravity (-)	Diolefins (wt.%)	Poly-substitute Aromatics (wt. %)	Cyclo-olefins (wt. %)	Bromine Index (g/100 g)	RON (-)
A23	360-D	113.32	0.76	1.30	19.56	0.02	27.86	87.93
	380	117.25	0.77	0.95	21.35	0.04	20.15	86.08
	360	110.56	0.76	2.17	20.13	0.09	39.15	87.58
A80	360-D	111.35	0.76	2.15	15.73	0.01	38.39	92.46
	380	111.71	0.76	1.94	22.00	0.01	35.48	86.56
	360	110.37	0.76	3.17	23.13	0.05	46.78	84.67
A117	360-D	114.06	0.77	2.16	23.89	0.03	34.13	82.60
	380	112.36	0.77	2.10	23.89	0.04	36.74	85.45
	360	112.47	0.77	2.60	26.64	0.04	39.98	84.88
AC23	360-D	113.78	0.76	1.28	13.80	0.00	30.73	87.96
	380	116.56	0.76	1.31	13.40	0.01	26.15	85.53
	340	118.07	0.78	2.00	26.77	0.02	27.46	81.89
	360	120.12	0.77	1.82	17.81	0.02	24.65	81.56
AC80	360-D	118.52	0.79	1.60	27.89	0.01	17.85	93.05
	380	118.27	0.77	1.78	17.64	0.02	28.07	86.55
	340	111.19	0.77	3.74	29.08	0.05	46.08	88.43
	360	121.60	0.78	1.93	28.47	0.02	19.42	91.09
AC117	360-D	111.11	0.76	2.49	22.90	0.02	41.47	90.51
	380	112.85	0.77	2.13	24.89	0.02	35.23	91.85
	340	114.56	0.77	2.92	26.87	0.04	38.75	83.82
	360	113.46	0.76	2.91	23.10	0.05	41.37	82.90
AC80_DB	360-D	107.93	0.76	5.41	24.02	0.06	42.24	83.38

5.2 Principal Component Analysis (PCA)

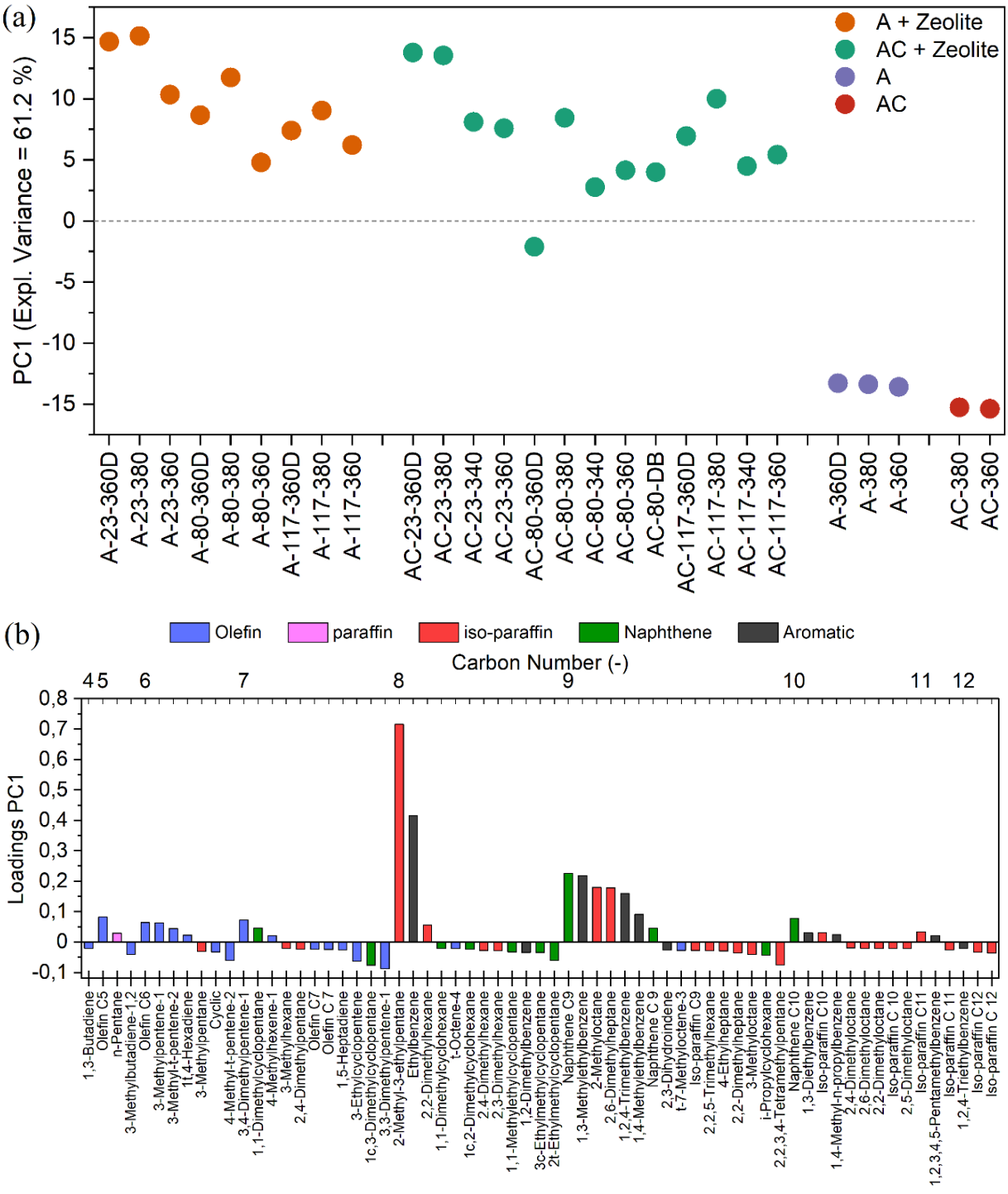

Figure S24. (a) PCA for all light oil samples with and without zeolites. (b) Loading for all HC evaluated in the PCA.

5.3 High-Performance Liquid Chromatography (HPLC)

Table S8. Normalized composition of oxygenated compounds in water detected via HPLC. Reaction conditions: 7 $NL \cdot gFe_3O_4^{-1} \cdot h^{-1}$ ($H_2/CO_2/N_2$ = 15/5/3), 360°C, 23 bar, 2 g Na/Fe_3O_4, 2 g zeolite.

Sample	Compound	A23	A80	A117	AC23	AC80	AC117	AC80_DB
Hot Water	Acetic acid	82.6%	86.2%	78.8%	92.9%	88.0%	89.8%	90.1%
	Propionic acid	12.5%	9.7%	8.9%	5.8%	8.8%	8.1%	7.6%
	Ethanol	0.0%	0.0%	0.0%	0.0%	0.0%	0.0%	0.0%
	Butanoic acid	5.0%	4.1%	12.3%	1.3%	3.2%	2.1%	2.3%
	2-propanol	0.0%	0.0%	0.0%	0.0%	0.0%	0.0%	0.0%
	1-propanol	0.0%	0.0%	0.0%	0.0%	0.0%	0.0%	0.0%
Cold Water	Acetic acid	15.2%	15.8%	20.6%	39.9%	20.7%	25.6%	28.5%
	Propionic acid	14.3%	9.3%	11.1%	11.2%	10.6%	11.5%	11.1%
	Ethanol	8.2%	3.1%	6.7%	3.6%	3.4%	10.1%	5.4%
	Butanoic acid	42.3%	52.5%	41.9%	33.7%	48.1%	40.6%	41.1%
	2-propanol	3.2%	0.0%	2.3%	0.0%	1.7%	0.0%	0.6%
	1-propanol	1.5%	2.8%	0.0%	0.0%	0.0%	0.0%	0.0%
	Butanone	15.3%	16.5%	17.4%	11.6%	15.5%	12.2%	13.3%

5.4 GC-MS Measurements

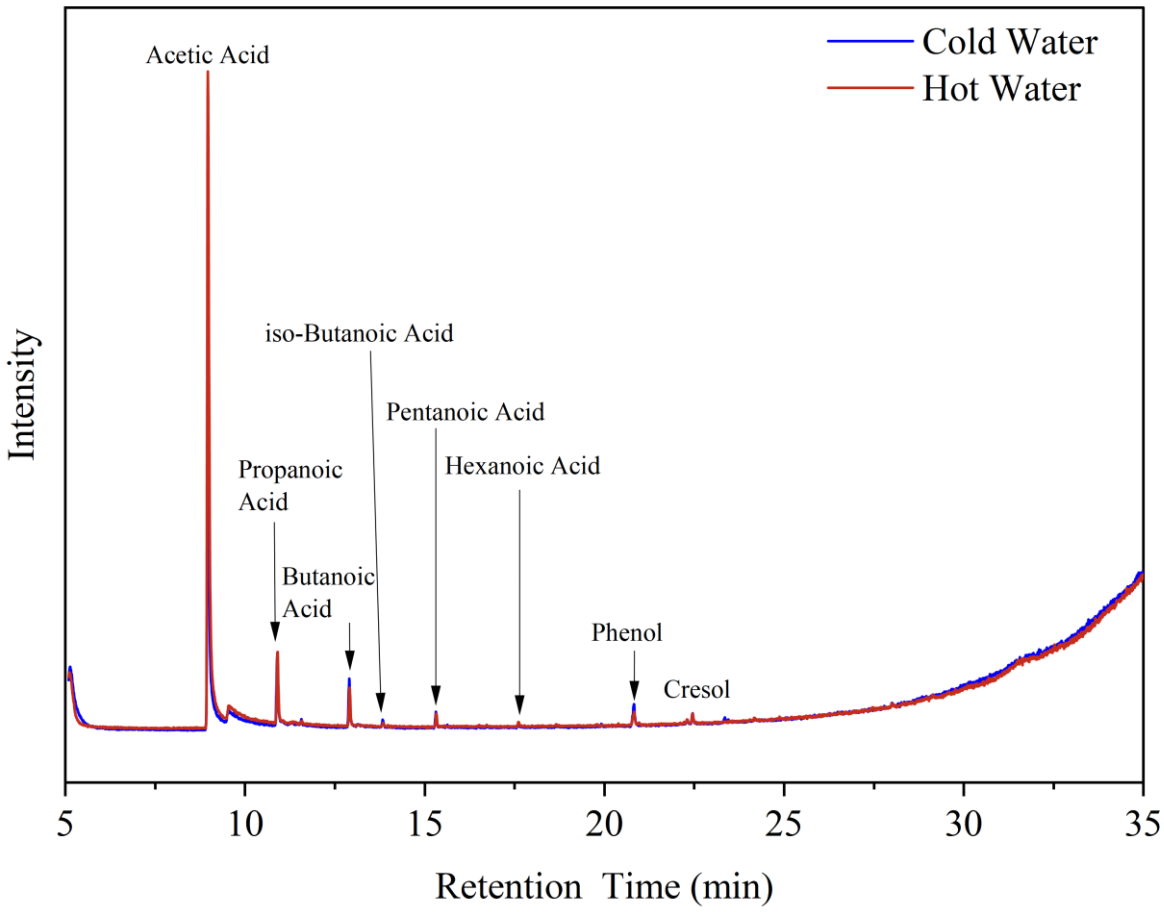

Figure S25. GC-MS profiles for hot and cold water of AC80 sample. Reaction conditions: 7 $NL \cdot gFe_3O_4^{-1} \cdot h^{-1}$ ($H_2/CO_2/N_2$ = 15/5/3), 360°C, 23 bar, 2 g Na/Fe_3O_4, 2 g zeolite.